JOURNAL OF ADVANCES IN MODELING EARTH SYSTEMS, VOL. 5, 1–7, doi:10.1002/jame.20049, 2013

The climate time scale in the approach to radiative-convective equilibrium

Timothy W. Cronin[1] and Kerry A. Emanuel[1]

Received 20 May 2013; revised 18 September 2013; accepted 19 September 2013.

[1] In this paper, we discuss the importance of the surface boundary condition (fixed versus interactive surface temperature) for the long time scale of approach to Radiative-Convective Equilibrium (RCE). Using a simple linearized two-variable model for surface-atmosphere interaction, we derive an analytic expression for τ_C, a long climate relaxation time scale that remains well defined and much longer than either mixing time scale of Tompkins and Craig (1998b), even in the limit that the heat capacity of the surface vanishes. We show that the size of τ_C is an intrinsic property of the coupling between the atmosphere and surface, and not a result of the thermal inertia of the surface alone. When the surface heat capacity is low, τ_C can be several times longer than expected, due to the effects of moisture on the effective heat capacity of the atmosphere. We also show that the theoretical expression for τ_C is a good predictor of best fit exponential relaxation time scales in a single-column model with full physics, across a range of surface temperatures and surface heat capacities.

Citation: Cronin, T. W., and K. A. Emanuel (2013), The climate time scale in the approach to radiative-convective equilibrium, *J. Adv. Model. Earth Syst.*, *5*, doi:10.1002/jame.20049.

1. Introduction

[2] Study of Radiative-Convective Equilibrium (RCE) has been foundational in our understanding of sensitivity and stability of planetary climates, and also forms the backbone of our understanding of the basic state of Earth's tropical atmosphere. The early studies of *Manabe and Strickler* [1964] and *Manabe and Wetherald* [1967], while simplistic in many ways, established quantitative estimates of the sensitivity of Earth's surface temperature to increased greenhouse gas concentrations that continue to be within the uncertainty ranges of modern general circulation models. In these studies, as well as others where changes in surface or near-surface air temperature are of primary concern, the surface temperature must be included as a prognostic variable, and surface energy balance must hold at equilibrium.

[3] In a different context, the basic state of the tropical atmosphere has often been characterized by the assumption of RCE. Especially with the growing ability to (marginally) resolve deep convection, and the influential papers of *Held et al.* [1993] and *Tompkins and Craig* [1998a], many studies of RCE and the tropical atmosphere have opted to fix the surface temperature as a boundary condition, rather than treat it as a prognostic variable. This means that surface energy balance no longer holds, since the surface implicitly acts as an energy source or sink that adjusts in magnitude exactly as needed to hold surface temperatures fixed. *Tompkins and Craig* [1998b] explored the importance of different time scales in RCE with a fixed surface temperature, and established the importance of two mixing time scales: a fast (∼2 day) time scale related to the cumulus updraft mass flux, and a slow (∼20 day) time scale governed by the radiative-subsidence speed and the depth of the convecting layer.

[4] However, the time scale of approach to RCE is much longer if the surface temperature is interactive. *Manabe and Wetherald* [1967] found relaxation time scales of ∼100 days, and pointed out that the approach to equilibrium at constant relative humidity takes longer than the approach at constant specific humidity, not only due to the impacts of water vapor as a greenhouse gas, but also to the internal latent energy of moist air. *Held and Suarez* [1974] noted that a fundamental time scale for equilibration of planetary climate is given by the "radiative relaxation time scale", $\tau_C = C/B$, where C is the heat capacity of a column of the atmosphere (units: J/m^2/K), and B is the change in the flux of net upward radiation at the top of the atmosphere per unit change in atmospheric temperature (units: W/m^2/K). The time scale τ_C may be increased by inclusion of the heat capacity of the mixed layer of the ocean, which

[1]Program in Atmospheres, Oceans, and Climate, Massachusetts Institute of Technology, Cambridge, Massachusetts, USA.

Corresponding author: T. W. Cronin, Program in Atmospheres, Oceans, and Climate, Massachusetts Institute of Technology, 77 Massachusetts Ave., Cambridge, Massachusetts 02139, USA. (twcronin@mit.edu)

1942-2466/13/10.1002/jame.20049

increases C, or by positive feedbacks in the climate system, which decreases B [*Held and Suarez*, 1974; *Wetherald and Manabe*, 1975]. While it may seem obvious that this climate time scale τ_C is the relevant relaxation time scale toward RCE with an interactive surface, this point appears rarely in discussions of RCE, and deserves to be made more explicitly. The size of τ_C relative to the time scales of *Tompkins and Craig* [1998b] is especially germane given recent studies with cloud-resolving models that have used interactive sea surface temperatures. Neither the study of *Romps* [2011] (which is well equilibrated), nor the study of *Khairoutdinov and Yang* [2013] (which is not), invoke τ_C as an explanation for the duration of a simulation that is required to reach equilibrium.

[5] The goal of this paper is thus to clarify more explicitly the scaling behavior of the time scale τ_C in RCE with an interactive surface. In section 2, we use a simple coupled two-variable surface-atmosphere model to derive τ_C, and show that it can easily be an order of magnitude larger than the slow mixing time scale of *Tompkins and Craig* [1998b]. We also find that the effective heat capacity of the atmosphere, C_A, which is relevant for the transition from one RCE state to another, can be considerably larger than the heat capacity of the dry troposphere, due to both internal latent energy and lapse rate considerations (section 2.1). In section 3, we perform simulations with a single-column model, and show that best fit relaxation time scales are predicted quite well by τ_C.

2. Theory

[6] To show that τ_C is a relevant time scale for a coupled atmosphere-surface system, we start from a simple two-variable model of atmosphere-surface interaction, which is linearized about a basic state that is in radiative-convective equilibrium (RCE, see the schematic in Figure 1). We construct perturbation equations for the temperature anomalies of the near-surface atmosphere, T'_A, and of the surface, T'_S, about basic-state values (T_A, T_S), assuming that C_A is the effective heat capacity of the troposphere, and that C_S is the heat capacity of the surface (both have units of J/m^2/K). We also assume that the tropospheric relative humidity stays roughly constant as the temperature of the troposphere changes, so that T'_A is accompanied by a boundary layer specific humidity perturbation $q' = T'_A \mathcal{H}(\partial q^*/\partial T)|_{T_A}$, where $\mathcal{H}$ is the near-surface relative humidity, and q^* is the saturation specific humidity. If the lower troposphere is opaque in the infrared, and the emission level for downwelling infrared radiation is close to the surface, then the linearization coefficients for the longwave radiative flux perturbation due to T'_A and T'_S are approximately equal in magnitude and opposite in sign. If we also follow *Barsugli and Battisti* [1998] and assume that the total surface latent plus sensible heat flux linearization coefficients are equal in magnitude and opposite in sign for T'_A and T'_S, then the total surface-atmosphere energy flux perturbation from the sum of changes in longwave radiation, plus latent and sensible turbulent exchange, can be parameterized by a single coefficient λ (units: W/m^2/K). The change in outgoing longwave radiation at the top of the atmosphere per unit change in surface air temperature (i.e., the inverse of the climate sensitivity) is given by the parameter B (units: W/m^2/K), which incorporates the water vapor feedback because of our assumption of constant relative humidity (the lower troposphere is opaque to longwave radiation, so T'_S does not directly affect the top-of-atmosphere energy balance). Finally, we assume minimal changes in shortwave radiative fluxes with temperature (e.g., no shortwave cloud-radiation feedbacks). Our equations for T'_A and T'_S are then given by:

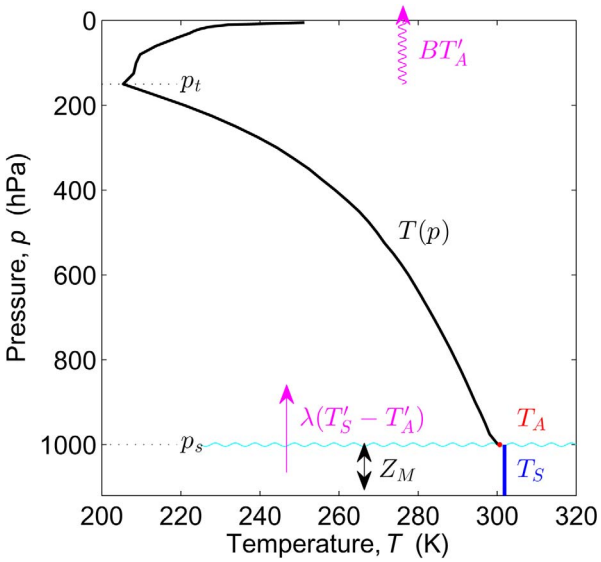

Figure 1. Schematic diagram of two-variable model for atmosphere-surface interaction in radiative-convective equilibrium. The surface air temperature, T_A, is the control variable for the atmosphere. Magenta lines indicate perturbation energy fluxes from the surface to the atmosphere, and from the atmosphere to space.

$$\begin{aligned} C_A \dot{T}'_A &= \lambda(T'_S - T'_A) - BT'_A \\ C_S \dot{T}'_S &= \lambda(T'_A - T'_S), \end{aligned} \tag{1}$$

where $\dot{x}$ denotes the time-derivative of x. Many of the assumptions in the derivation of (1) have been made for the purposes of the simplicity of subsequent algebra, and the general conclusions are robust to a more complex linearization that allows for shortwave cloud feedbacks, coefficients for perturbation latent heat flux that are unequal in magnitude, and a lower troposphere that is nonopaque in the infrared. The application of (1) in the presence of cloud radiative feedbacks will be discussed briefly in section 4.

[7] If either T'_A or T'_S is fixed in (1), the relaxation time scales are very simple. If T'_S is held fixed, then T'_A decays toward $[\lambda/(\lambda+B)]T'_S$ with a time scale τ_A:

$$\tau_A = C_A/(\lambda + B). \tag{2}$$

[8] On the other hand, if T'_A is held fixed, then T'_S decays toward T'_A with a time scale τ_S:

$$\tau_S = C_S/\lambda. \tag{3}$$

[9] The coupled system can be expressed in matrix form as:

$$\begin{bmatrix} \dot{T}'_{\mathrm{A}} \\ \dot{T}'_{\mathrm{S}} \end{bmatrix} = \begin{pmatrix} -1/\tau_A & \eta/\tau_A \\ 1/\tau_S & -1/\tau_S \end{pmatrix} \times \begin{bmatrix} T'_A \\ T'_S \end{bmatrix}, \tag{4}$$

where η is the nondimensional ratio $\lambda/(\lambda + B)$. The relaxation time scales of the coupled system (1) are given by the eigenvalues r of the matrix in (4):

$$2r = -\left(\frac{1}{\tau_A} + \frac{1}{\tau_S}\right) \pm \left[\left(\frac{1}{\tau_A} + \frac{1}{\tau_S}\right)^2 - 4\frac{1-\eta}{\tau_A \tau_S}\right]^{1/2}. \tag{5}$$

[10] Both values of r are negative and real, so the system is stable and nonoscillatory; the longer relaxation time scale τ_C corresponds to the smaller absolute value of r ($\tau_C = |r|^{-1}$), which occurs for the $+\sqrt{()}$ solution. Since the second term in the discriminant in (5) is much smaller in magnitude than the first, the binomial approximation can be applied to the radical; along with replacement of $(1-\eta)^{-1}$ with $(\lambda + B)/B$, this results in a great deal of simplification:

$$\tau_C \approx \frac{\lambda + B}{B}(\tau_A + \tau_S). \tag{6}$$

[11] It is worth noting that the long time scale τ_C is strictly greater than the sum of the two time scales $\tau_A + \tau_S$, and is typically larger by an order of magnitude; taking $\lambda \sim 40\mathrm{W/m^2/K}$, and $B \sim 2\mathrm{W/m^2/K}$ [e.g., *Nilsson and Emanuel*, 1999], we would have $\tau_C = 21(\tau_A + \tau_S)$. The mode of variability that experiences this long decay timescale corresponds to same-signed and nearly equal perturbations in T_A and T_S; the more rapidly damped mode (which we will not discuss) corresponds to opposite-signed perturbations in T_A and T_S, which have nearly equal magnitudes of stored energy. Although it may appear from (6) that τ_C depends strongly on λ, plugging in (2) and (3) reveals that:

$$\tau_C = B^{-1}(C_A + C_S) + \lambda^{-1} C_S. \tag{7}$$

[12] In general, $\lambda \gg B$, so τ_C can be approximated as $(C_A + C_S)/B$.

2.1. Effective Tropospheric Heat Capacity

[13] The impacts of moisture can make C_A several times larger than the dry heat capacity of the troposphere, and can thus lead to a large increase in τ_C as temperature increases. The dry heat capacity of the troposphere is given by:

$$C_{A,\mathrm{dry}} = c_p(p_s - p_t)/g, \tag{8}$$

where p_s is the surface pressure, p_t the tropopause pressure, and c_p is the specific heat of dry air at constant pressure. For a tropopause around 200 hPa, $C_{A,\mathrm{dry}} \approx 8.2\times10^6\mathrm{J/m^2/K}$. However, (1) was based on energy conservation, so a more rigorous definition of C_A is given by:

$$C_A \equiv \frac{\partial\langle k\rangle}{\partial T_A}, \tag{9}$$

where $\langle k\rangle$ is the tropospheric integral of the moist enthalpy (units: $\mathrm{J/m^2}$):

$$\langle k\rangle = \int_{p_t}^{p_s} (c_p T + L_v q)\, dp/g = \langle c_p T\rangle + \langle L_v q\rangle. \tag{10}$$

[14] As recognized by the early study of *Manabe and Wetherald* [1967], the assumption of constant relative humidity results in a substantial increase in C_A, because the latent heat capacity of the troposphere, $\partial\langle L_v q\rangle/\partial T_A$, can be large compared to $C_{A,\ \mathrm{dry}}$, especially at warm temperatures. We can estimate the magnitude of the latent heat capacity of the troposphere by multiplying a typical tropical value of column water vapor $\langle q\rangle \sim 50\,\mathrm{kg/m^2}$ by L_v and by the fractional rate of change of specific humidity with temperature, $\sim$7%/K, which gives $\partial\langle L_v q\rangle/\partial T_A \approx 8.75\times10^6\mathrm{J/m^2/K}$. For tropical temperatures, the latent heat capacity of the troposphere can be comparable to, or larger than, the dry heat capacity of the troposphere.

[15] We can decompose the latent heat capacity of the troposphere into two components: the first is related to changes in saturation specific humidity with temperature, and the second is related to changes in relative humidity with temperature. As in *Bretherton et al.* [2005], we define $\overline{\mathcal{H}}$ as the column relative humidity:

$$\overline{\mathcal{H}} = \langle q\rangle/\langle q^*\rangle, \tag{11}$$

or ratio of total column water vapor, $\langle q\rangle$, to that of a saturated column, $\langle q^*\rangle$. Then the latent heat capacity of the troposphere can be expressed as:

$$\frac{\partial\langle L_v q\rangle}{\partial T_A} = L_v\langle q^*\rangle\frac{\partial\overline{\mathcal{H}}}{\partial T_A} + L_v\overline{\mathcal{H}}\frac{\partial\langle q^*\rangle}{\partial T_A}, \tag{12}$$

where we have additionally assumed that the effects of temperature on L_v can be neglected.

[16] Tropospheric moisture also has another consequence that is significant for our understanding of C_A. By constraining the thermal structure of the troposphere to be roughly moist-adiabatic, moist convection amplifies temperature changes in the upper troposphere, relative to temperature changes at the surface. If we define $\overline{T}$ as the mass-weighted average temperature of the troposphere, then $\partial\overline{T}/\partial T_A > 1$; the magnitude of this effect is more difficult to estimate, but

Table 1. Table of Equilibria for RC Model Simulations Across the Range of Insolation Values[a] $\overline{I}$

$\overline{I}$ (W/m^2)	T_A (°C)	OLR (W/m^2)	p_t (hPa)	$\overline{\mathcal{H}}$ (%)	B (W/m^2/K)	$\frac{\delta\overline{T}}{\delta T_A}$ (i)	$\frac{L_v\langle q^*\rangle\delta\overline{\mathcal{H}}}{C_{A,\mathrm{dry}}\delta T_A}$ (ii)	$\frac{L_v\overline{\mathcal{H}}\delta\langle q^*\rangle}{C_{A,\mathrm{dry}}\delta T_A}$ (iii)	$\frac{L_v\delta\langle q\rangle}{C_{A,\mathrm{dry}}\delta T_A}$ (iv)	$\frac{C_A}{C_{A,\mathrm{dry}}}$ (v)	C_A (10^7J/m^2/K)
290	−1.03	232.6	325	61.6							
300	2.81	241.1	300	58.6	2.22	1.13	−0.02	0.15	0.13	1.26	0.90
310	6.73	249.9	275	60.1	2.25	1.19	0.02	0.20	0.21	1.40	1.04
320	9.75	258.5	275	59.0	2.84	1.25	−0.02	0.26	0.24	1.49	1.11
330	11.8	266.9	250	56.7	4.18	1.36	−0.07	0.32	0.24	1.60	1.23
340	14.7	275.3	225	52.7	2.81	1.39	−0.10	0.36	0.26	1.65	1.31
350	19.3	284.2	200	53.2	1.98	1.48	0.01	0.48	0.49	1.97	1.62
360	26.1	293.9	150	62.5	1.42	1.53	0.22	0.79	1.01	2.54	2.21
370	32.5	303.0	100	67.3	1.42	1.51	0.20	1.35	1.55	3.06	2.82

[a]Equilbria are a function of $\overline{I}$ only; C_S affects the relaxation time scale but not the properties of the equilibria. Values in row j for B, C_A, and terms in columns (i–v), are computed based on finite differences (denoted with δ symbols) between equilibrium states for rows j and $j-1$ (e.g., $B_j=(\mathrm{OLR}_j-\mathrm{OLR}_{j-1})/(T_{Aj}-T_{Aj-1})$). Columns labeled (i–v) are based on the decomposition of $C_A/C_{A,\,\mathrm{dry}}$ given in (13).

$\partial\overline{T}/\partial T_A$ also generally increases at warmer temperatures. Taken together with the impacts of tropospheric latent heat capacity (12), the upper-tropospheric amplification of temperature changes implies that:

$$C_A = C_{A,\mathrm{dry}}\left(\frac{\partial\overline{T}}{\partial T_A}+\frac{L_v\langle q^*\rangle}{C_{A,\mathrm{dry}}}\frac{\partial\overline{\mathcal{H}}}{\partial T_A}+\frac{L_v\overline{\mathcal{H}}}{C_{A,\mathrm{dry}}}\frac{\partial\langle q^*\rangle}{\partial T_A}\right), \quad (13)$$

where we have normalized all terms by the dry heat capacity of the troposphere ($C_{A,\,\mathrm{dry}}$). We will use equation (13) to diagnose the relative importance of different aspects of moisture for the effective tropospheric heat capacity in our simulations with a radiative convective model; note that it is only approximate when differentials are replaced by finite differences, since we have ignored correlations between changes in $\overline{\mathcal{H}}$ and changes in $\langle q^*\rangle$. In practice, however, this missing correlation term is negligible. Also, the assumption of constant relative humidity in our derivation of τ_C may seem inconsistent with our allowance for changes in relative humidity in (13), but in practice there is little contradiction because changes in relative humidity are quite small.

3. Single-Column Simulations

[17] To test our theoretical expression for the long time scale of approach to RCE with an interactive surface, we conduct simulations with the single-column model of *Renno et al*. [1994] (using the convection scheme of *Emanuel and Zivkovic-Rothman* [1999]) across a range of solar insolation values $\overline{I}$ and surface heat capacities C_S. We will express the surface heat capacity in terms of the depth of an equivalent mixed layer of liquid water, Z_M; $C_S=c_l Z_M$, where c_l is the volumetric heat capacity of liquid water, $\approx 4.2\times10^6$J/m^3/K. A mixed layer with $Z_M\approx$ 2m has about the same heat capacity as the dry troposphere (as given by $C_{A,\,\mathrm{dry}}$). For all simulations, we use a CO_2 concentration of 300 ppm, a surface albedo of 0.2, and a fixed solar zenith angle whose cosine is 2/3 (equal to the planetary-average, insolation-weighted value). The model has 46 levels in the vertical (tropospheric resolution of 25 hPa), and a time step of 5 min. For simplicity, we perform simulations without cloud-radiation interactions.

[18] We first use the RC model to obtain equilibrium soundings, then we perturb the insolation and study the relaxation toward new equilibria. Initial equilibria are calculated from 4000 day simulations with $\overline{I}=(290, 300, 310, 320, 330, 340, 350, 360, 370)\mathrm{W/m}^2$. We perturb each sounding by adding 10 W/m^2 to the initial insolation, and calculate the best fit relaxation time scale τ_R toward the new equilibrium temperature T_f, from an initial temperature T_i, using a three-parameter exponential curve fit in MATLAB $\left(T_\mathrm{A}(t)=T_\mathrm{f}+(T_\mathrm{i}-T_\mathrm{f})\times e^{-t/\tau_R}\right)$. For each choice of insolation, we perform perturbation simulations across a range of $Z_M=$ (0.5, 1.0, 2.5, 4.0, 5.0, 6.0, 7.5, 10.0, 15.0, 20.0) m.

[19] The set of chosen insolation values results in simulated surface air temperatures that range from slightly below 0°C to slightly over 30°C (Table 1 describes the equilibria, and will be discussed over the course of this section). The relaxation time scale fit from RC model perturbation experiments can be as large as several hundred days even when $Z_M=0.5$ m, and generally increases with both T_A and Z_M (Figure 2). One of the most striking features of Figure 2 is the large local minimum in relaxation time scale for $T_A\approx 10-15^\circ$C. This minimum in τ_R occurs because B, as diagnosed from model output, is a local maximum there (Table 1). We suspect that this reflects a numerical issue related to the lack of variability in the model, and the related constraint that important transition levels (e.g., tropopause, boundary layer top) must change in discrete jumps. Regardless of whether the variations in B have physical or numerical origins, they result in real changes in the relaxation time scales of the model.

[20] We diagnose values of B and C_A based on finite differences in temperature, column relative humidity, saturation specific humidity, and outgoing longwave radiation between RC model equilibrium states (see Table 1). The theoretical scaling $\tau_C\approx(C_A+C_S)/B$ compares well with best fit RC model relaxation time scales τ_R, with an R^2 value of 0.95 for a $\tau_C=\tau_R$ fit

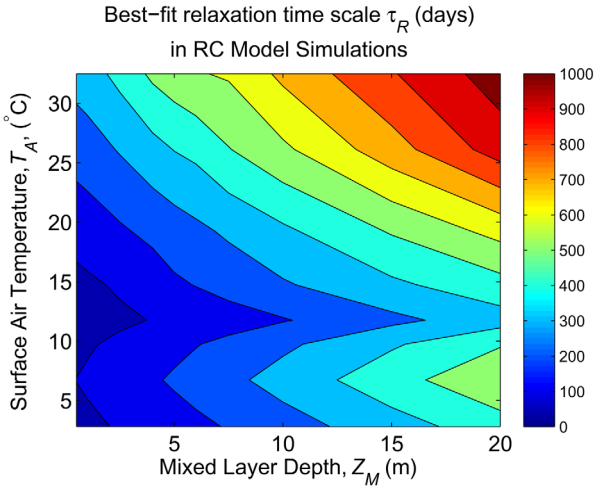

Figure 2. Contour plot of best fit relaxation time scale in days, from RC model simulations.

(Figures 3 and 4). Figures 3 and 4 show that the theory (τ_C) slightly underestimates best fit RC model timescales (τ_R), on average. Neglect of the term C_S/λ (from (7)) in our simplification of $\tau_C \approx (C_A+C_S)/B$ goes in the right direction, but not far enough, to eliminate the underestimate. Invalidity of the assumptions of the theory, or biased estimation of B and C_A, provide possible reasons for the slight underestimation of τ_R by τ_C. Since the theory captures the bulk of the variance in the relaxation time scale as T_A and C_S are varied, exploration of the small deviations of τ_C from τ_R is left as a topic for future study.

[21] How important are increases in atmospheric heat capacity (C_A) relative to increases in climate sensitivity (B^{-1}) for the increases in relaxation timescale (τ_R) at very warm temperatures? What are the largest contributors to the systematic increase in atmospheric heat

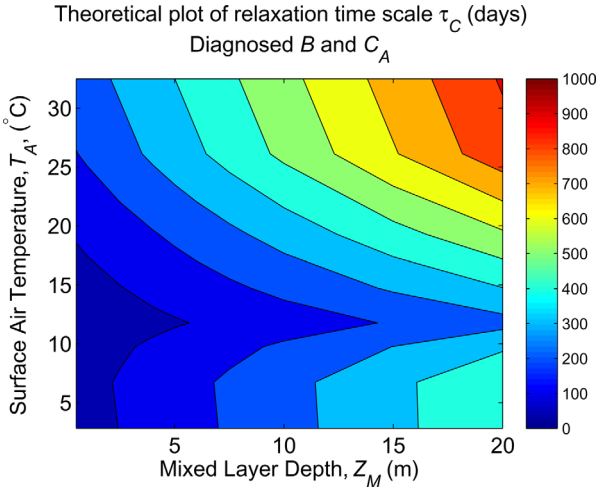

Figure 3. Contour plot of theoretical relaxation time scales in days, based on values of B and C_A as diagnosed from RC model simulations (see Table 1 for values of B and C_A as a function of T_A).

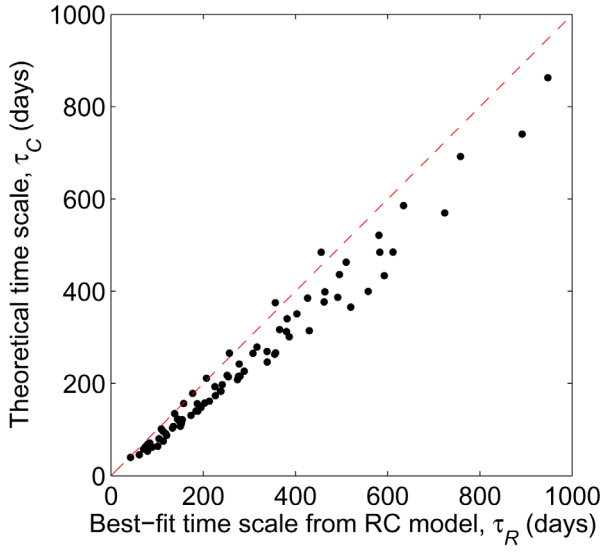

Figure 4. Scatter plot of theoretical versus best fit RC model relaxation time scales (i.e., results from Figures 2 and 3), in days. Red dashed line indicates the 1–1 line; $R^2 = 0.95$ for the model-theory fit.

capacity with temperature? Columns (i)–(iii) of Table 1 decompose C_A into the three terms of equation (13) (normalized by $C_{A,\,\mathrm{dry}}$). Column (iv) represents the normalized latent heat capacity of the troposphere, equal to the sum of columns (ii) and (iii), plus the residual term involving correlation between changes in $\overline{\mathcal{H}}$ and changes in $\langle q^* \rangle$; this residual term is very small, with magnitude at most $0.01 C_A/C_{A,\mathrm{dry}}$. Column (v) represents the normalized total heat capacity of the troposphere, or sum of columns (i) and (iv). We see that the dominant contribution to increases in $C_A/C_{A,\,\mathrm{dry}}$ at very warm temperatures is due to changes in $\langle q^* \rangle$ with T_A, and that changes in column relative humidity are generally a much smaller term than changes in column-integrated saturation specific humidity (see columns (ii) versus (iii) in Table 1). For a range of moderate temperatures, ~5–20°C, lapse rate effects contribute most to the elevated values of $C_A/C_{A,\mathrm{dry}}$; $(\partial\overline{T}/\partial T_A - 1)$ is larger than the normalized latent heat capacity of the troposphere (see columns (i) versus (iv) in Table 1). The tropospheric heat capacity is also affected by changes in $C_{A,\,\mathrm{dry}}$, which occur due to the increase in tropospheric mass as the tropopause rises with warmer temperatures; tropopause pressure p_t is diagnosed as the first level in the model, going upward, where the time-mean radiative cooling rate is less than 0.05 K/day. Taken in isolation, changes in tropospheric mass are a small factor, but since they multiply the ratio $C_A/C_{A,\,\mathrm{dry}}$, they have a magnified influence. From the coldest to the warmest equilibria, C_A increases by a factor of 3.13, with $C_A/C_{A,\,\mathrm{dry}}$ increasing by a factor of 2.43, and tropospheric mass increasing by a factor of 1.29. Changes in B are markedly less important than changes in C_A for the systematic increase of τ_C with T_A. For the coldest simulations, $B \approx 2.2\mathrm{W/m^2/K}$, while for the warmest simulations, $B \approx 1.4\mathrm{W/m^2/K}$. Thus increases

in B^{-1} only serve to increase τ_C by a factor of $\sim$1.5. For low C_S, increases in C_A with increasing temperature are the dominant contributor to the lengthening of τ_C with warming, specifically due to the large sensitivity of $\langle q^* \rangle$ to changes in T_A.

4. Discussion and Conclusions

[22] We have attempted to clarify that the long time scale of approach to radiative-convective equilibrium with an interactive surface is given by $\tau_C \approx (C_A + C_S)/B$. A close examination of the problem reveals some interesting nuances, especially related to the magnitude of the effective atmospheric heat capacity relative to its dry value. Simulations with a single-column model show good agreement with the theoretical time scale, and highlight our finding that long time scales are not a result of the thermal inertia of the surface alone. A warm atmosphere in RCE has considerable thermal inertia on its own, and can have a relaxation time scale as large as several hundred days even as $C_S \to 0$.

[23] Although we have not explicitly considered cloud-radiation interactions, which are important in many recent studies of radiative-convective equilibrium, the results from the theory turn out to be rather flexible to changes in structural assumptions. Cloud longwave feedbacks could be incorporated into B without any changes to the structure of the theory at all. Cloud shortwave feedbacks would introduce an additional term, DT'_A, into the equation for the evolution of T'_S. This term introduces additional algebra and notation, but so long as D is small compared to $\lambda, \tau_C \approx (C_A + C_S)/(B - D)$, where $(B - D)$ is a climate sensitivity parameter that incorporates the impact of clouds on shortwave radiation.

[24] The findings from this paper should help to clarify the length of a simulation that is needed to reach equilibrium with an interactive surface temperature. As found by *Khairoutdinov and Yang* [2013], even the ability to perform simulations with a 3-D cloud-resolving model for 700 days may not be enough to reach equilibrium with an interactive surface. Since τ_C is a function of both the climate sensitivity, B^{-1}, and the tropospheric heat capacity, C_A, which both generally vary among models, a precise estimate of τ_C depends on the specific behavior of a given model. But determination of B for a given model also seems to require several long simulations with interactive T_S across a range of forcing conditions. As noted by *Held et al.* [1993], in principle one can resolve this conundrum by conducting simulations across a range of fixed T_S values, and studying the dependence of the net energy flux into the surface on the surface temperature. In practice, this approach seems to be underused as a means of characterizing the sensitivity of 3-D cloud-resolving models. Our work points to the value of this approach, even if the ultimate goal is to conduct simulations with an interactive surface.

[25] It is possible that the long relaxation time scale, τ_C, has implications for the interpretation or understanding of climate variability, which have not been fully considered. The two-variable model we have used is very similar to that of *Barsugli and Battisti* [1998], who explored the importance of atmosphere-ocean coupling for the redness of the spectrum of midlatitude climate variability. More recently, and with application to the tropics, *Clement et al.* [2011] suggested that a dynamically active ocean is not necessary to produce interannual to decadal-time scale variability in the tropical Pacific; an "ENSO-like" mode of tropical Pacific climate variability appears to operate in many thermally coupled atmosphere-slab ocean models independent of any ocean dynamical response. If variability in the zonal location of convection and T_S anomalies is only weakly damped by heat export to the extratropics, then our work suggests that a null model for such a mode may not need to even invoke large-scale atmospheric dynamics; the long decorrelation time and red spectrum found by *Clement et al.* [2011] for thermally coupled atmosphere-slab ocean models may simply be related to the size of τ_C.

[26] The increase in effective atmospheric heat capacity as temperatures warm may also be relevant to understanding recent findings that global warming can lead to delayed monsoon onset, and an increased lag in the seasonal cycle of tropical precipitation relative to the seasonal cycle of insolation [*Bordoni and Merlis*, 2013; *Dwyer et al.*, 2013]. Other things equal, we would expect increased atmospheric heat capacity with warmer temperatures to lead to an increase in the lag between peak solar forcing and peak large-scale ascent and rainfall. The dependence of C_A on temperature may thus provide a simple thermodynamic mechanism to explain delayed monsoon onset in a warmer climate. Clearly, many of the assumptions of our theory may break down when applied to the seasonal cycle (e.g., seasonal changes in temperature may not occur with a moist-adiabatic vertical structure); we simply wish to suggest here the possibility that systematic changes in tropospheric heat capacity with temperature may be important for understanding the response of the seasonal cycle to climate change.

[27] A final open question relates to the time scales of approach to equilibrium for a coupled surface-atmosphere model where the atmospheric column is constrained by the weak temperature gradient (WTG) approximation [*Sobel et al.*, 2001]. A better understanding of the time scales in the WTG atmosphere-land system could be particularly relevant for the important problem of understanding persistence time scales of precipitation anomalies over tropical land.

[28] **Acknowledgments.** Thanks to Peter Molnar for comments on a draft of this work, to Martin Singh for helpful conversations, and to two anonymous reviewers for useful comments. This work was funded by NSF grant 1136480, The Effect of Near-Equatorial Islands on Climate.

References

Barsugli, J., and D. Battisti (1998), The basic effects of atmosphere-ocean thermal coupling on midlatitude variability, *J. Atmos. Sci.*, *55*, 477–493.

Bordoni, S., and T. Merlis (2013), Response of aquaplanet monsoons to changes in longwave radiation, paper presented at 19th Conference on Atmospheric and Oceanic Fluid Dynamics, Am. Meteorol. Soc., Newport, Rhode Island, 17 Jun.

Bretherton, C., P. Blossey, and M. Khairoutdinov (2005), An energy-balance analysis of deep convective self-aggregation above uniform SST, *J. Atmos. Sci.*, *62*, 4273–4292, doi:10.1175/JAS3614.1.

Clement, A., P. DiNezio, and C. Deser (2011), Rethinking the ocean's role in the southern oscillation, *J. Clim.*, *24*, 4056–4072, doi:10.1175/2011JCLI3973.1.

Dwyer, J., M. Biasutti, and A. Sobel (2013), The effect of greenhouse-gas-induced changes in SST on the seasonality of tropical precipitation, paper presented at 6th Northeast Tropical Workshop, SUNY Albany, Rensselaersville, New York, 29 May.

Emanuel, K., and M. Zivkovic-Rothman (1999), Development and evaluation of a convection scheme for use in climate models, *J. Atmos. Sci.*, *56*, 1766–1782.

Held, I., and M. Suarez (1974), Simple albedo feedback models of the icecaps, *Tellus*, *26*, 613–629.

Held, I., R. Hemler, and V. Ramaswamy (1993), Radiative-Convective equilibrium with explicit two-dimensional moist convection, *J. Atmos. Sci.*, *50*, 3909–3927.

Khairoutdinov, M., and C.-E. Yang (2013), Cloud resolving modelling of aerosol indirect effects in idealised radiative-convective equilibrium with interactive and fixed sea surface temperature, *Atmos. Chem. Phys.*, *13*, 4133–4144, doi:10.5194/acp-13-4133-2013.

Manabe, S., and R. Strickler (1964), Thermal equilibrium of the atmosphere with a convective adjustment, *J. Atmos. Sci.*, *21*, 361–385.

Manabe, S., and R. Wetherald (1967), Thermal equilibrium of the atmosphere with a given distribution of relative humidity, *J. Atmos. Sci.*, *24*, 241–259.

Nilsson, J., and K. Emanuel (1999), Equilibrium atmospheres of a two-column radiative-convective model, *Q. J. R. Meteorol. Soc.*, *125*, 2239–2264.

Renno, N., K. Emanuel, and P. Stone (1994), Radiative-convective model with an explicit hydrologic cycle. I: Formulation and sensitivity to model parameters, *J. Geophys. Res.*, *99*, 14,429–14,441.

Romps, D. (2011), Response of tropical precipitation to global warming, *J. Atmos. Sci.*, *68*, 123–138, doi:10.1175/2010JAS3542.1.

Sobel, A., J. Nilsson, and L. Polvani (2001), The weak temperature gradient approximation and balanced tropical moisture waves, *J. Atmos. Sci.*, *58*, 3650–3665.

Tompkins, A., and G. Craig (1998a), Radiative-convective equilibrium in a three-dimensional cloud-ensemble model, *Q. J. R. Meteorol. Soc.*, *124*, 2073–2097.

Tompkins, A., and G. Craig (1998b), Time-scales of adjustment to radiative-convective equilibrium in the tropical atmosphere, *Q. J. R. Meteorol. Soc.*, *124*, 2693–2713.

Wetherald, R., and S. Manabe (1975), The effects of changing the solar constant on the climate of a general circulation model, *J. Atmos. Sci.*, *32*, 2044–2059.